Cell Death and Differentiation (2006) 13, 499–511

www.nature.com/cdd

Sodium orthovanadate suppresses DNA damage-induced caspase activation and apoptosis by inactivating p53

A Morita*[,1,2,6], J Zhu[2,6], N Suzuki[1,2,3], A Enomoto[2,4], Y Matsumoto[2,4], M Tomita[2], T Suzuki[4], K Ohtomo[4,5] and Y Hosoi[2,4]

[1] Department of Radiological Health, Graduate School of Medicine, University of Tokyo, Tokyo 113-0033, Japan
[2] Department of Radiation Oncology, Graduate School of Medicine, University of Tokyo, Tokyo 113-0033, Japan
[3] Department of Radiological Sciences, School of Health Science, International University of Health and Welfare, Tochigi 324-8501, Japan
[4] Department of Radiation Research, Center for Disease Biology and Integrative Medicine, Graduate School of Medicine, University of Tokyo, Tokyo 113-0033, Japan
[5] Department of Radiology, Graduate School of Medicine, University of Tokyo, Tokyo 113-0033, Japan
[6] These authors contributed equally to this work
* Corresponding author: A Morita, Department of Radiological Health, Graduate School of Medicine, University of Tokyo, 7-3-1 Hongo, Bunkyo-ku, Tokyo 113-0033, Japan. Tel: +81 3 5841 3505; Fax: +81 3 5841 3013; E-mail: morita@m.u-tokyo.ac.jp

Received 03.3.05; revised 07.7.05; accepted 01.8.05; published online 02.9.05
Edited by C Prives

Abstract

We previously reported that p42/SETβ is a substrate for caspase-7 in irradiated MOLT-4 cells, and that treating the cells with sodium orthovanadate (vanadate) inhibits p42/SETβ's caspase-mediated cleavage. Here, we initially found that the inhibitory effect of vanadate was due to the suppression of caspase activation but not of caspase activity. Further investigations revealed that vanadate suppressed upstream of apoptotic events, such as the loss of mitochondrial membrane potential, the conformational change of Bax, and p53 transactivation, although the accumulation, total phosphorylation, and phosphorylation of six individual sites of p53 were not affected. Importantly, vanadate suppressed p53-dependent apoptosis, but not p53-independent apoptosis. Finally, gel-shift and chromatin immunoprecipitation assays conclusively demonstrated that vanadate inhibits the DNA-binding activity of p53. Vanadate is conventionally used as an inhibitor of protein tyrosine phosphatases (PTPs); however, we recommend that the influence of vanadate not only on PTPs but also on p53 be considered before using it.

Cell Death and Differentiation (2006) **13,** 499–511.
doi:10.1038/sj.cdd.4401768; published online 2 September 2005

Keywords: sodium orthovanadate; p53; caspase; DNA damage; apoptosis

Abbreviations: vanadate, sodium orthovanadate; ChIP, chromatin immunoprecipitation; PTP, protein tyrosine phosphatase; IR, irradiation; Cyt.*c*, cytochrome *c*; Smac/DIABLO, second mitochondria-derived activator of caspase/direct IAP-binding protein with low pI; $\Delta\psi$m, mitochondrial membrane potential; PUMA, p53 upregulated modulator of apoptosis; DTT, dithiothreitol; DMHV, *bis*(*N,N*-dimethylhydroxamido) hydrooxovanadate; DPS, 3,4-dephostatin; PAO, phenylarsine oxide; Z-VAD-FMK, Z-Val-Ala-Asp(OMe)-CH_2F; MOLT/mBcl-2, MOLT-4 cells overexpressing the murine Bcl-2; MOLT/Nega, MOLT-4 cells that overexpress a negative control shRNA; PI, propidium iodide; mAb, monoclonal antibody; RNA pol II, RNA polymerase II; S.D., standard deviation

Introduction

The human T-cell leukemia cell line MOLT-4 is hypersensitive to X-irradiation (IR). Irradiated MOLT-4 cells show apoptotic cell death characterized by nuclear condensation and DNA fragmentation mediated by activated caspases.[1–4] Recent studies by us and others have demonstrated that the p53 and SAPK/JNK pathways are involved in the radiation-induced MOLT-4 apoptosis.[1–3] In our previous studies, we reported the induction of a new protein, p41, in this apoptotic process. p41 is induced after IR through cleavage of p42/SETβ and appears to be a specific catalytic product of caspase-7 and a marker of apoptosis.[4,5]

Caspases are a family of aspartate-specific cysteine proteases activated during apoptosis, and are normally present in cells as proenzymes that require limited proteolysis for the activation of enzymatic activity. Activated caspases precipitate the irreversible commitment of the cell to apoptotic death by cleaving a number of substrates, many of which have been identified. Caspases are classified into two types: initiator and effector caspases. Enzymatic activation of initiator caspases, such as caspase-8 and -9, leads to proteolytic activation of downstream effector caspases, which include caspase-3, -6, and -7. For instance, the fact that either caspase-9 deficiency or apoptotic protease activating factor-1 (Apaf-1) deficiency results in resistance to the apoptosis induced by ionizing radiation or other DNA-damaging agents indicates that these agents preferentially activate the caspase-9/Apaf-1/cytochrome *c* (Cyt.*c*)-dependent apoptotic pathway. In this activation of caspase-9, the release of Cyt.*c* from the mitochondria into the cytosol acts as a trigger for the formation of the caspase-9/Apaf-1/Cyt.*c* complex called the apoptosome and initiates the caspase cascade. In addition, second mitochondria-derived activator of caspase/direct IAP-binding protein with low pI (Smac/DIABLO), another released mitochondrial protein, enhances the enzymatic activity of caspases by obstructing the association of the IAPs (inhibitors of apoptosis proteins) with the caspases. Overexpressing antiapoptotic Bcl-2 family members inhibits the release of Cyt.*c* and Smac/DIABLO and related events such as the

conformational change of Bax and the loss of mitochondrial membrane potential ($\Delta\psi$m).[6–9]

p53 is a well-studied transcription factor associated with the cell's decision between apoptosis and other fates after DNA damage. After DNA damage, p53 stability is increased by phosphorylation, and the accumulated p53 induces the transcription of its target genes.[10] Overexpressing a dominant-negative form of p53 in MOLT-4 cells results in resistance to radiation-induced apoptosis.[1] Recent studies have revealed two potential mediators of p53-dependent apoptosis, p53 upregulated modulator of apoptosis (PUMA)[11] and Histone H1 (especially Histone H1.2).[12] Once transactivated by p53, they cause the release of mitochondrial proapoptotic molecules into the cytosol and initiate the caspase cascade.

Vanadate (sodium orthovanadate, Na_3VO_4) is widely used as an inhibitor of protein tyrosine phosphatases (PTPs).[13] In our research, vanadate was originally found to be an inhibitor of p41 induction in irradiated MOLT-4 cells, although this induction is mediated by caspase-7.[4,5] The objective of this study was to clarify the effect of vanadate, and we speculated that the inhibitory effect of vanadate on the cleavage of p42/SETβ to p41 would be due to suppression of either the activation or the activity of caspases. Therefore, we investigated the effect of vanadate on caspases and related apoptotic processes. We conclude that vanadate suppresses caspase activation by acting on the upstream process of caspase activation, that is, its transactivation by p53.

Results

Vanadate suppresses caspase activation and apoptosis in irradiated MOLT-4 cells

We initially investigated the effect of vanadate on recombinant caspase-7 activity *in vitro*. Figure 1a shows that vanadate had little effect on the activity of recombinant caspase-7, even when dithiothreitol (DTT), an antioxidant that enhances caspase activity, was absent from the reaction buffer. Therefore, we next investigated the effect of vanadate on caspase activation. At 800 μM, vanadate almost completely suppressed the activation of caspase family members including caspase-7, and prevented the release of Cyt.*c* and Smac/DIABLO into the cytosol (Figure 1b). These results were in agreement with the suppression of radiation-induced MOLT-4 apoptosis at 800–1600 μM by vanadate, with tolerable cytotoxicity (Figure 1c). We also examined the antiapoptotic effect of several known PTP inhibitors on this apoptosis (Figure 1c, right panel). We found that a vanadate compound, *bis*(*N,N*-dimethylhydroxamido) hydrooxovanadate (DMHV),[14] that permeates cell membranes more easily than vanadate does, also suppressed the apoptosis, whereas the other inhibitors, 3,4-dephostatin (DPS) and phenylarsine oxide (PAO), did not. In particular, PAO was very cytotoxic for the MOLT-4 cells. The concentrations of DPS and PAO in these experiments were sufficient to inhibit PTPs.[15,16] Accordingly, the suppressive effect of the vanadate compounds was unlikely to be related to their inhibitory activity against PTPs, because not all the PTP inhibitors tested inhibited the apoptosis.

Vanadate acts upstream of the caspase activation and the release of mitochondrial proapoptotic molecules into the cytosol

We further investigated the effects of vanadate, and compared them with those of a caspase inhibitor or overexpressed Bcl-2. As shown in Figure 2a, the release of mitochondrial proapoptotic molecules into the cytosol was suppressed by a caspase inhibitor, Z-Val-Ala-Asp(OMe)-CH_2F (Z-VAD-FMK) or overexpressed Bcl-2 (MOLT-4 cells overexpressing the murine Bcl-2 (MOLT/mBcl-2)), as well as by vanadate. However, the suppressive effects of vanadate on the mitochondrial release and the cell death required that the vanadate be given sooner after IR treatment than Z-VAD-FMK. Figure 2b and c show that the effectiveness of giving vanadate diminished progressively and was abolished by 3 h after IR, whereas Z-VAD-FMK was still effective when given 4 h after the IR treatment. Since the release starts 5 h after IR (data not shown), Z-VAD-FMK is effective until just before the release. These results suggest that the Z-VAD-FMK affects the mitochondrion itself and that vanadate may act on apoptotic processes that precede the release.

To pursue this idea further, we next investigated the effect of vanadate on events prior to the release, that is, the conformational change of Bax and loss of $\Delta\psi$m. In the experiments on Bax, an anti-Bax antibody was used as a probe for conformationally changed Bax, because the changed Bax exposes its antigenic epitope in nondenaturing conditions.[9] As shown in Figure 3a, the fluorescence intensity of Bax increased after IR, while the amount of Bax protein analyzed by denaturing gel immunoblotting did not (Figure 3b). Figure 3a shows that the change was suppressed by vanadate or overexpressed Bcl-2 but not by Z-VAD-FMK. Similar results were obtained in the analysis of the loss of $\Delta\psi$m (Figure 3c). These data demonstrate that vanadate acts on the events upstream of the release and that Z-VAD-FMK inhibits the release steps.

Vanadate suppresses p53-dependent DNA damage-induced apoptosis

We further investigated the effect of vanadate on DNA damage-induced apoptosis in several cell lines. Interestingly, the suppression of this apoptosis occurred exclusively among three wild-type p53 cell lines and not in two p53-null cell lines (Figure 4a and b).[1,17–20] It is known that these three cell lines show p53-dependent apoptosis when stimulated by DNA-damaging agents.[1,17,18] In fact, these wild-type p53 cell lines showed the activation (accumulation) of p53 after the DNA-damaging treatments, and, as expected, the two p53-null cell lines did not (Figure 4d). Unlike the wild-type p53 cell lines, the two p53-null cell lines were more susceptible to X-rays when treated with vanadate than when they were exposed to X-rays alone, and high concentrations of vanadate alone were sufficient to induce apoptosis in these lines (Figure 4b). In addition, vanadate enhanced the apoptosis induced by anisomycin, which activates SAPK/JNK and does not activate p53 in MOLT-4 cells[3] (Figure 4c). These data suggest that vanadate antagonizes p53 functions and stimulates the

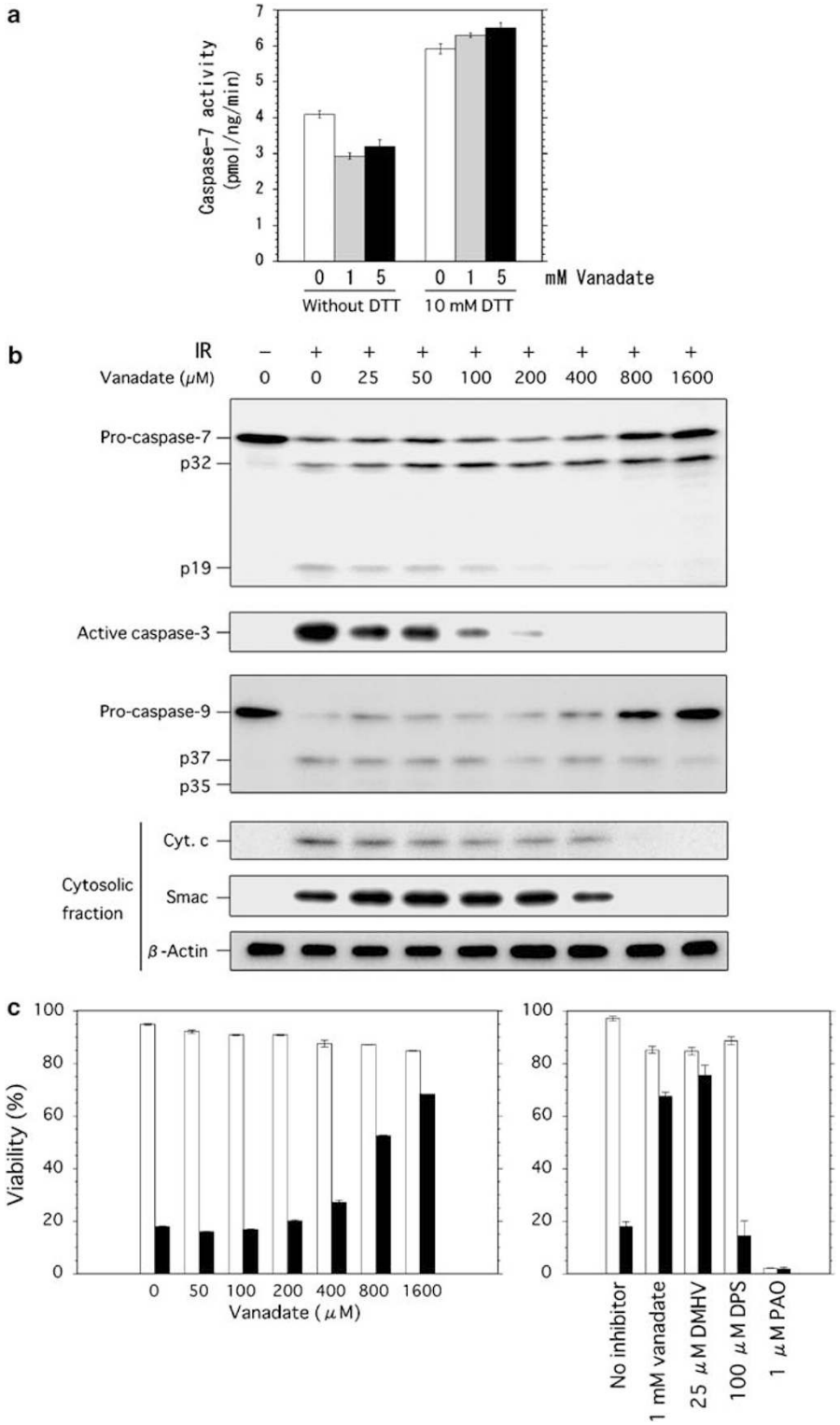

Figure 1 Vanadate suppresses caspase activation and apoptosis in irradiated MOLT-4 cells. (**a**) Vanadate does not suppress recombinant caspase-7 activity. Caspase-7 activity was assayed as described in Materials and Methods. (**b**) Dose dependency of the suppressive effect of vanadate on the release of mitochondrial proapoptotic molecules into the cytosol and on caspase activation in irradiated MOLT-4 cells. Cells were harvested 10 or 7 h after 10 Gy IR for measurements of caspase activation or the released proapoptotic molecules, respectively. Proteins were detected by immunoblotting. (**c**) Cell viabilities were quantified by staining with Annexin V-FITC plus PI and by flow cytometric analysis. Open bars indicate the viabilities of unirradiated samples 18 h after treatment, and closed bars indicate the viabilities of 10 Gy-irradiated samples 18 h after treatment. Left panel: dose dependency of the suppressive effect of vanadate on radiation-induced apoptosis of MOLT-4. Right panel: comparison of the antiapoptotic effect of several known PTP inhibitors on the radiation-induced apoptosis of MOLT-4. Data shown are means ± standard deviation (S.D.) from three to five independent experiments

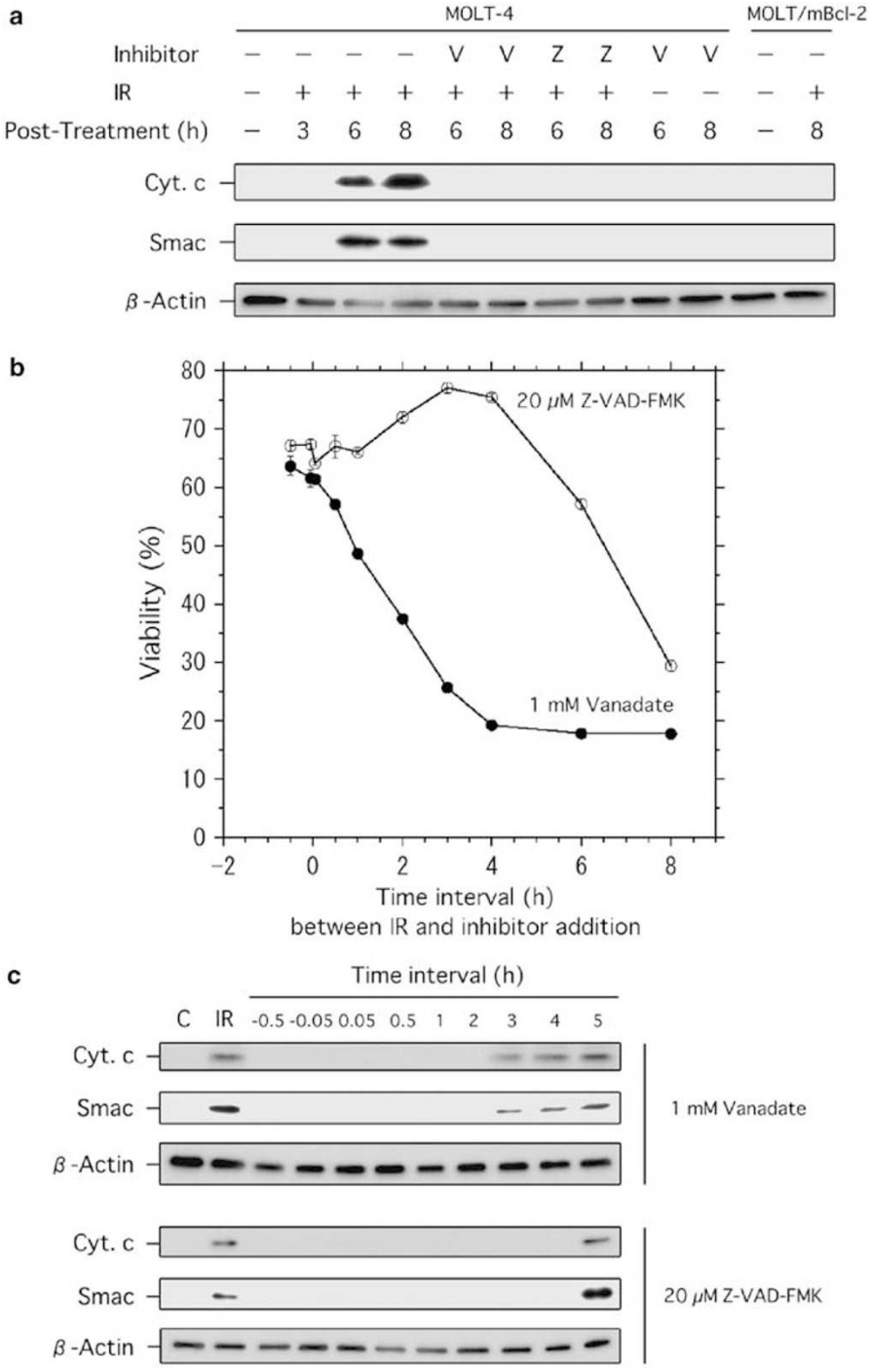

Figure 2 Vanadate requires earlier administration than a caspase inhibitor to suppress apoptosis in irradiated MOLT-4 cells. (**a**) Treatment with a caspase-inhibitor, Z-VAD-FMK, or overexpressed Bcl-2 suppressed the radiation-induced release of Cyt.*c* and Smac/DIABLO from MOLT-4 mitochondria. In all, 10 Gy-irradiated MOLT-4 cells treated with 1 mM vanadate (V) or 20 μM Z-VAD-FMK (Z), and 10 Gy-irradiated MOLT/mBcl-2 cells were collected at the indicated times, and then subjected to subcellular fractionation and immunoblotting. (**b**, **c**) Each horizontal axis represents the time interval between the 10 Gy IR and the addition of the inhibitor. MOLT-4 cells were harvested 18 h (**b**) or 7 h (**c**) after IR for viability determination or measurements of the released proapoptotic molecules, respectively. The cell viabilities shown in (**b**) were quantified by staining with AnnexinV-FITC plus PI and by flow cytometric analysis. Data shown are means $\pm$ S.D. from three independent experiments

SAPK/JNK pathway. Furthermore, using a vector that overexpressed p53 siRNA, we generated two stable p53-knockdown transformants (MOLT/p53KD-1, -2). These clones showed almost undetectable levels of p53 expression even after IR, and were resistant to radiation-induced apoptosis (Figure 4d and e). Vanadate did not suppress the slow decreases in cell viability following IR in these lines, but a mock transfectant (MOLT-4 cells that overexpress a negative

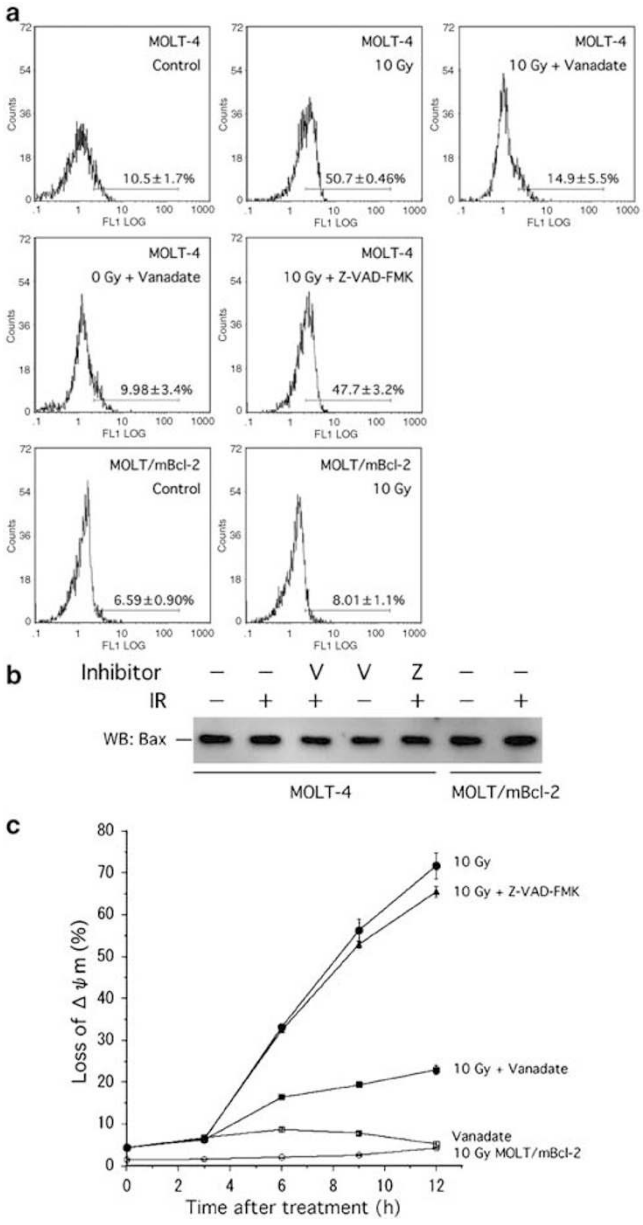

Figure 3 Vanadate suppresses the conformational change of Bax and the loss of mitochondrial potential in irradiated MOLT-4 cells. Vanadate (V) and Z-VAD-FMK (Z) were used at final concentrations of 1 mM and 20 μM, respectively. (**a**) The conformational change of Bax measured by anti-Bax immunoreactivity. Cells were harvested 5 h after treatment. (**b**) The amount of Bax protein did not change 5 h after IR and/or vanadate treatment when analyzed by immunoblotting with the same antibody used in (**a**). (**c**) The loss of $\Delta\psi$m in irradiated MOLT-4 cells measured with a flow cytometer after MitoTracker staining. Data shown in (**a**) and (**c**) are representative of at least three independent experiments

control shRNA (MOLT/Nega)) showed similar p53 accumulation and viability curves after treatments as the parental cells. Interestingly, like the p53-null cell lines, these knockdown transfectants were more susceptible to X-rays when treated with vanadate than when they were exposed to X-rays alone (Figure 4e). These data probably indicate vanadate's specificity for p53 in suppressing DNA damage-induced apoptosis, and suggest that the loss of p53 functions enhances vanadate's cytotoxic side effect(s).

We next investigated the effects of vanadate on p53 transactivation after IR. We found that vanadate almost completely suppressed the induction of two p53 target gene products, p21 and PUMA, at 800 μM, although the accumulation of p53 was not affected by vanadate (Figure 5a). The same lack of effect of vanadate on p53 accumulation was found in the three wild-type p53 cell lines tested (Figure 4d). On the other hand, overexpressed Bcl-2 did not suppress the induction of these genes (Figure 5b). The suppression by vanadate was also verified by RT-PCR analysis of the transcription of *p21* and *puma* (Figure 5c). Similar results were obtained in the analysis of the release of nuclear Histone H1 into the cytosol (Figure 6).

Vanadate induces inactivation of p53 and inhibits its DNA-binding activity

We next examined the phosphorylation status of p53 using a [^{32}P]-labeling experiment, and by immunoblotting with phospho-p53-specific antibodies and a phosphotyrosine antibody. In the [^{32}P]-labeling experiment, although p53 was induced by the radioactivity of $H_3^{32}PO_4$ (Figure 7a, 1st lane), vanadate did not affect the total phosphorylation level of p53 (Figure 7a). We next investigated the effect of vanadate on several known individual phosphorylation sites.[10] We found that the phosphorylation of p53 on Ser6, Ser9, Ser15, Ser20, Ser46, or Ser392 was not affected by vanadate (Figure 7b). We also considered the effect on p53 of vanadate's inhibiting PTPs. This activity might have caused irregular tyrosine phosphorylation of p53 (human p53 contains nine tyrosine residues in its 393-amino-acid sequence[21]), although p53 is not known to be modified by phosphorylation on tyrosine. To verify this assumption, and moreover, to ascertain the total tyrosine-phosphorylation state of MOLT-4 cells treated with vanadate, we investigated the tyrosine phosphorylation state of p53 and MOLT-4 cells by immunoblotting using a phosphotyrosine antibody, 4G10 monoclonal antibody (mAb). Figure 7c shows that tyrosine-phosphorylated p53 was undetectable in any sample (lanes 6–9), although the total tyrosine phosphorylation increased slightly in irradiated MOLT-4 cells treated with vanadate (lanes 3–5). These data increase the likelihood that there are other causes of vanadate's effects on p53 than the alteration of p53 phosphorylation, even though these findings do not completely rule out the possibility that p53 is modified at other Ser/Thr phosphorylation sites.

Thus, to pursue other possibilities, we examined the effects of vanadate on the conformation of p53 using the anti-p53 PAb 240 mAb as a probe for the inactivated form of p53.[22–24] In nondenaturing conditions, PAb 240 mAb recognizes the inactivated form of p53 but not the normal form, whereas the DO-1 mAb recognizes both forms. PAb 240 mAb immunoprecipitated the p53 from irradiated MOLT-4 cells treated with vanadate but not from cells exposed to X-rays alone (Figure 8a). These data indicate that vanadate induces the inactivation of p53. We next investigated the effect of vanadate on the DNA-binding activity of p53 by means of gel-shift assays. We found that, although vanadate decreased the amount of nuclear p53 a little, the vanadate-induced inhibition of p53's DNA-binding activity had a larger effect (Figure 8b). These results indicated that vanadate weakly

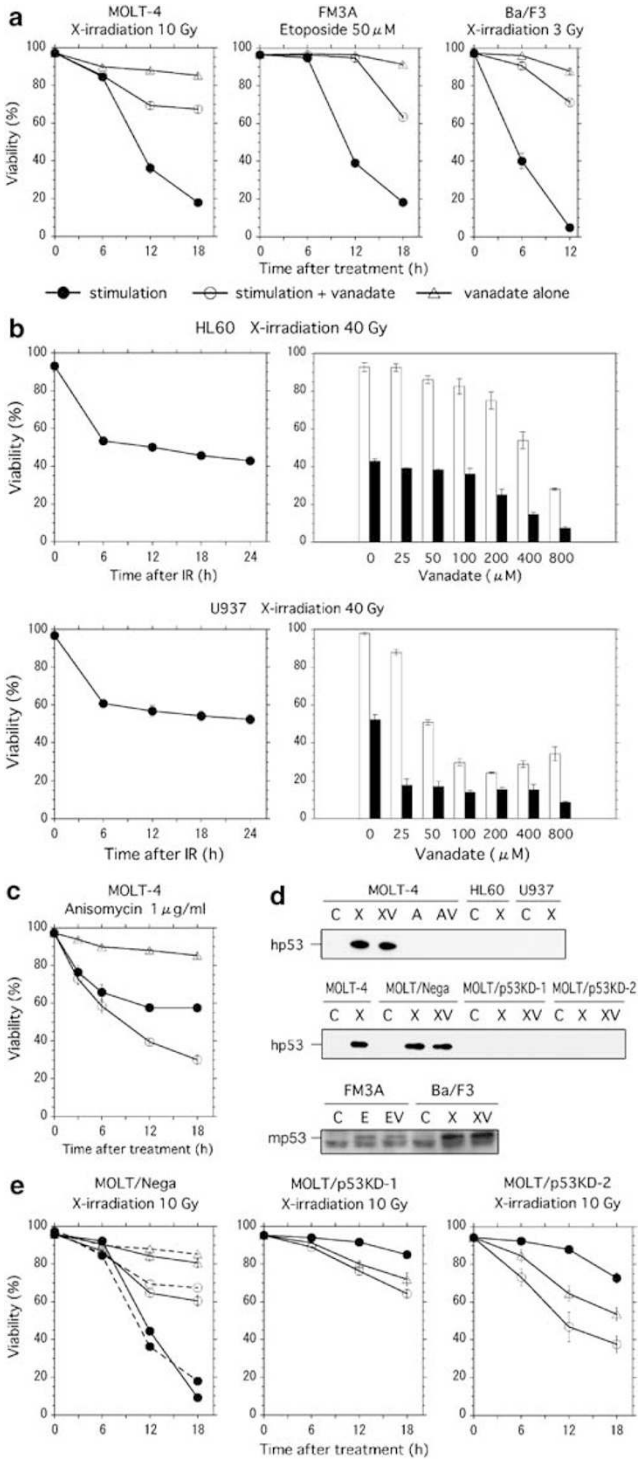

Figure 4 Vanadate suppresses p53-dependent DNA damage-induced apoptosis. Cell viabilities were quantified by staining with AnnexinV-FITC plus PI and by flow cytometric analysis. (**a**), (**c**)–(**e**) The concentrations of vanadate used here were 1 mM for X-irradiated MOLT-4 cells, 100 μM for FM3A cells treated with etoposide, 800 μM for X-irradiated Ba/F3 cells, 1 mM for MOLT-4 cells treated with anisomycin, and 1 mM for X-irradiated MOLT-4 stable transformants (MOLT/Nega, and MOLT/p53KD-1, -2), respectively. (**a**), (**b**) (Left panel), (**c**), (**e**) symbols represent viabilities as follows: closed circles, stimulation alone; open circles, stimulation with vanadate; open triangles, vanadate alone. (**b**) Vanadate does not suppress the radiation-induced apoptosis of the two p53-null cell lines. Right panel: open bars indicate the viabilities of unirradiated samples with various concentrations of vanadate 24 h after treatment, and closed bars indicate the viabilities of irradiated samples with various concentrations of vanadate 24 h after treatment. Data shown are the means $\pm$ S.D. from three to five independent experiments. (**d**) Treatments were as follows, cell lines are given in parentheses: C, control. (MOLT-4 and MOLT-4 stable transformants) X, 10 Gy IR; XV, 10 Gy IR plus 1 mM vanadate; A, 1 μg/ml anisomycin; AV, 1 μg/ml anisomycin plus 1 mM vanadate. (HL60 and U937) X, 40 Gy IR. (FM3A) E, 50 μM etoposide; EV, 50 μM etoposide plus 100 μM vanadate. (Ba/F3) X, 3 Gy IR; XV, 3 Gy IR plus 800 μM vanadate. Cells were harvested 6 h after treatments, and p53 was detected by immunoblotting (hp53, human p53; mp53, murine p53). (**e**) MOLT/Nega: dashed lined viability curves represent the parental MOLT-4 cells' viability curves as indicated in (**a**)

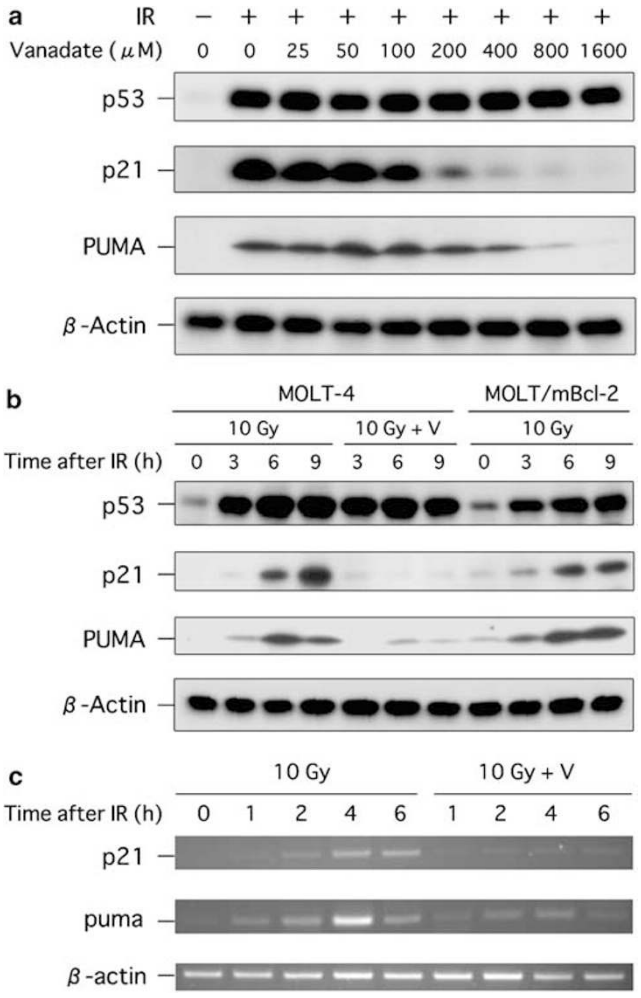

Figure 5 Vanadate suppresses the transactivation of p53 target genes but not the accumulation of p53. (**a**) The effect of vanadate on the accumulation of p53 and the induction of p53 target gene products, p21 and PUMA. Cells were harvested 6 h after 10 Gy IR, and the proteins were detected by immunoblotting. (**b**) Time course of the accumulation of p53 and the induction of p21 and PUMA in irradiated MOLT-4 cells with or without vanadate (1 mM) and in irradiated MOLT/mBcl-2 cells. Proteins were detected by immunoblotting. (**c**) RT-PCR analysis of transcription of *p21* and *puma* in irradiated MOLT-4 cells in the presence or absence of vanadate (1 mM)

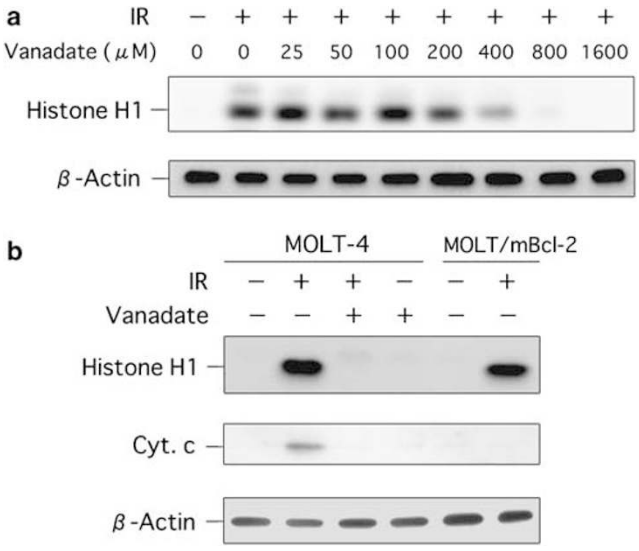

Figure 6 Vanadate suppresses the p53-dependent release of Histone H1 into the cytosol. Cytosolic proteins were detected by immunoblotting. (**a**) Dose dependency of the suppressive effect of vanadate on the release of Histone H1 into the cytosol in irradiated MOLT-4 cells. Cytosolic samples were the same as used in Figure 1b. (**b**) Overexpressed Bcl-2 cannot suppress the release of Histone H1. The samples (6 h after 10 Gy IR) were the same as used in Figure 2a

inhibits the nuclear localization of p53, and potently inhibits the DNA-binding activity of p53. The slight decrease in the nuclear retention of p53 may be associated with the inhibition of p53's DNA-binding activity.

To compare the DNA-binding activity by equivalent concentrations of p53 from untreated or vanadate-treated irradiated cells, the amounts of DNA-bound *versus* input p53 were plotted as binding curves (Figure 8c). The binding curves indicated that the rabbit polyclonal antibody used in the super-shift assays activated the DNA-binding activity of p53 to a certain degree, and that, even in the super-shift assays, the DNA-binding activity of p53 from vanadate-treated irradiated cells was lower than the binding activity of p53 from the cells exposed to X-rays alone, at all amounts of input p53 tested. We also ascertained the inactivation by vanadate of intracellular p53's DNA binding to its target promoters by means of chromatin immunoprecipitation (ChIP) assays (Figure 8d). Vanadate and DMHV inhibited the DNA binding of p53 to the *p21* and *puma* promoters at 800 and 25 μM, respectively. In addition, the data shown in Figures 5a and 8d indicate that vanadate treatment leads to a more severe inhibitory effect on *p21* than on *puma*. However, the antiapoptotic effect of vanadate probably correlates with *puma* suppression and not with *p21* suppression, since this effect appeared markedly at 800 μM (Figure 1c).

Finally, to determine whether this effect was direct or not, we used recombinant p53 on gel-shift assays. Figure 8e indicates that vanadate and DMHV could directly inhibit the DNA-binding activity of p53. We found that these two compounds showed a similar inhibition pattern in this experiment. Both inhibitors completely abrogated the DNA-binding activity of recombinant p53 at 3 mM, and significant inhibition was obtained at concentrations of 1 mM and lower (vanadate, 1 mM, 300 μM, and 100 μM: 98, 78, and 75% inhibition, respectively; DMHV, 1 mM, 300 μM, and 100 μM: 95, 86, and 58% inhibition, respectively, estimated by densitometry). Interestingly, 30 μM DMHV did not inhibit the DNA-binding activity of p53 (Figure 8e), whereas 25 μM DMHV inhibited DNA-binding activity of intracellular p53 (Figure 8d). The data shown in Figure 8d (*in vivo*) and Figure 8e (*in vitro*) indicate that the effective concentration of the two inhibitors was much the same *in vitro*, and that DMHV was more effective *in vivo* than *in vitro*.

Discussion

In this study, we demonstrate that vanadate is a chemical inhibitor of p53 that inactivates its DNA-binding activity. We

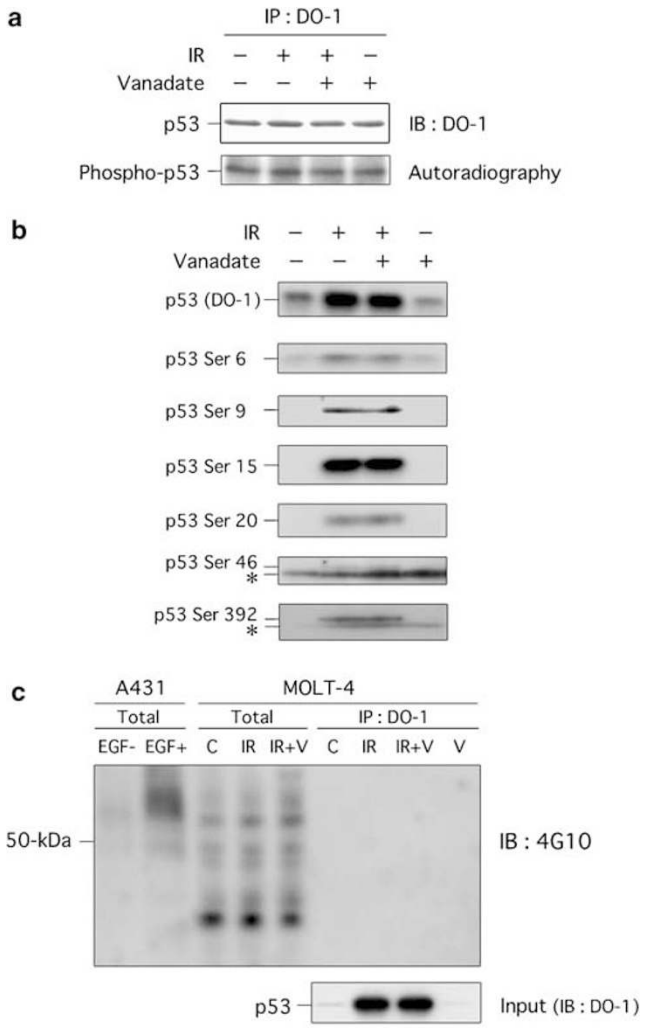

Figure 7 Vanadate does not alter the extent of total phosphorylation or the individual phosphorylation of six sites of p53. (**a**) Immunoprecipitation of [^{32}P]-labeled p53 using anti-p53 DO-1 mAb to investigate the effect of vanadate on the total phosphorylation of p53. MOLT-4 cells were harvested 6 h after treatment (10 Gy IR and/or 1 mM vanadate). Immunoprecipitated p53 and phospho-p53 were visualized by immunoblotting (IB) and autoradiography, respectively. (**b**) Evaluation of p53 phosphorylation at multiple sites using rabbit polyclonal antibodies against the phosphorylated residues Ser6, Ser9, Ser15, Ser20, Ser46, and Ser392. MOLT-4 cells were harvested 6 h after treatment (10 Gy IR and/or 1 mM vanadate). Asterisks indicate nonspecific bands. (**c**) Immunoblotting using phosphotyrosine antibody (4G10) against the DO-1-immunoprecipitated p53. Cell lysates from A431 cells cultured for 20 min in the absence (1st lane) or presence (2nd lane) of 50 ng/ml EGF were used as the negative and positive control, respectively. The 4G10 mAb detected the upregulation of tyrosine phosphorylation in EGF-stimulated A431 cells. MOLT-4 cells were harvested 6 h after treatment (10 Gy IR and/or 1 mM vanadate). The amount of the input immunoprecipitated p53 was determined by immunoblotting using Anti-p53 DO-1 mAb

initially investigated the effect of vanadate on caspases. We found that vanadate suppressed caspase activation and the subsequent cell death, but did not suppress caspase activity. We further investigated vanadate's effect on upstream apoptotic events, such as the loss of $\Delta\psi$m, the conformational change of Bax, and p53 transactivation. We found that vanadate suppressed all these events except for the accumulation of p53, its total phosphorylation status, and the phosphorylation status of the residues we investigated. Finally, we identified vanadate as an inhibitor of p53 by comparing its effect on p53-dependent apoptosis with its effect on p53-independent apoptosis, by immunoblotting and RT-PCR analysis of p53 transactivation, by immunoprecipitation analysis that was based on activation-status differences in p53 immunoreactivity, by ChIP assays, and by gel-shift assays. We conclude that vanadate largely inhibits transcription by p53 through the direct inactivation of its DNA-binding activity.

As an aside, our results suggest the possibility that Z-VAD-FMK has an inhibitory effect on the mitochondrial permeability transition (Figure 2). Alternatively, Z-VAD-FMK may inhibit only caspases, and the initial activation of the caspases may be upstream of the release, resulting in the inhibition of the release. Recent studies have shown cases that require caspase activation before mitochondrial permeabilization.[25] Further study to assess whether caspase activation precedes the release of proapoptotic molecules into the cytoplasm in irradiated MOLT-4 cells is needed to distinguish between these possibilities; however, there is no doubt that Z-VAD-FMK does not inhibit upstream events such as the loss of $\Delta\psi$m and the conformational change of Bax (Figure 3).

Although vanadate has a variety of biological effects, it has been widely used as an inhibitor of PTPs.[13] However, the fact that not all PTP inhibitors suppress the MOLT-4 apoptosis suggests that this effect of vanadate is unrelated to its PTP inhibition activity (Figure 1c). Moreover, MOLT-4 cells treated with vanadate showed only a slight upregulation of their total tyrosine phosphorylation (Figure 7c). Our results indicate that the cellular concentration of vanadate used in this study was insufficient to inhibit PTPs, but was sufficient to inhibit transcription by p53. Therefore, the influence of vanadate on p53 should be considered, even in experiments where it is used as a PTP inhibitor. On the other hand, it is known that vanadate is not very membrane permeable.[14] The low permeability of vanadate was also observed in our study. For example, a membrane-permeable form of vanadate, DMHV, suppressed the apoptosis and *puma* induction at 25 μM, whereas vanadate required an approximately 30- to 40-fold higher concentration to obtain the same effect (Figures 1c and 8d). The increased effectiveness of DMHV is in agreement with the first study of DMHV in cells.[14] However, we do not simply interpret these data to mean that the actual intracellular concentration of vanadate required to inhibit p53 is approximately 25 μM, because 30 μM vanadate (data not shown) and DMHV (Figure 8e) did not inhibit the DNA-binding activity of p53 *in vitro*. To obtain over 50% inhibition of p53's DNA-binding activity by either compound required concentrations of 100 μM and above *in vitro* (Figure 8e). The similarity of the *in vitro* effectiveness of the two compounds on purified PTP was also described previously.[14] Therefore, we believe that the actual cellular concentration of vanadate required to suppress p53 and apoptosis is in the several hundred-micromolar range, and that the effect of DMHV may involve several factors besides membrane permeability, such as the metabolism, incorporation, exclusion, or accumulation of DMHV in cells.

Many researchers have also described the effects of vanadate on apoptosis; however, this issue is controversial

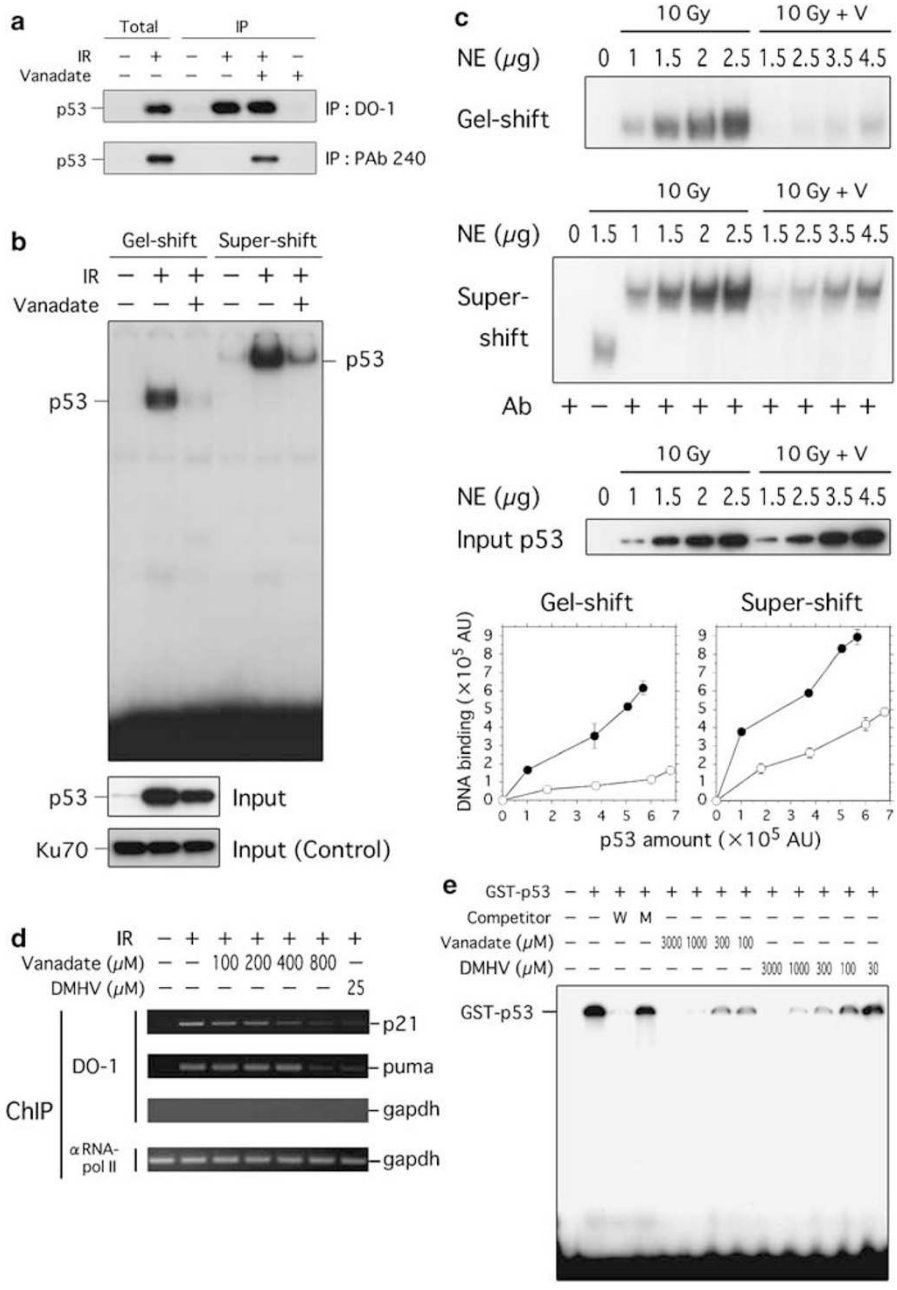

Figure 8 Vanadate inhibits the DNA-binding activity of p53. (**a**) Immunoprecipitation of p53 using anti-p53 DO-1 mAb (upper panel) and PAb 240 mAb (lower panel). PAb 240 mAb recognized p53 in 10 Gy-irradiated MOLT-4 cells treated with vanadate (1 mM) but not in the cells exposed to X-rays alone (6 h after IR). Total cell lysates from unirradiated (1st lane) or 10 Gy-irradiated (2nd lane) MOLT-4 cells cultured for 6 h were used, respectively, as the negative and positive controls for p53. The p53 from total cell lysates (lanes 1 and 2) and the immunoprecipitated p53 (lanes 3 to 6) were visualized by immunoblotting using anti-p53 DO-1 mAb. (**b**) MOLT-4 cells were 10 Gy-irradiated and treated with or without vanadate (1 mM). Nuclear extracts were prepared 4 h after IR. Left three lanes: a gel-shift assay. Right three lanes: a super-shift assay using a rabbit polyclonal antibody against amino-acid residues 367–381 of human p53. The amount of p53 and Ku70 (as an internal control) in input nuclear extracts (2.5 μg) was determined by immunoblotting. Vanadate decreased the amount of nuclear p53 a little, while the levels of Ku70 were unchanged by vanadate. (**c**) Comparison of the DNA-binding activity of p53 between untreated and vanadate-treated irradiated MOLT-4 cells. Each input p53 from nuclear extract (NE) was visualized by immunoblotting using the anti-p53 DO-1 mAb. The signal intensities were quantified by densitometry, and plotted in arbitrary units (AU) as binding curves (bottom graphs). Symbols represent the amount of DNA binding as follows: Closed circles, IR alone; open circles, IR with vanadate. Data shown in (**c**) are representative of at least three independent experiments. (**d**) Effect of vanadate or DMHV on the *in vivo* p53's DNA binding to the *p21*, *puma*, and *gapdh* (as a negative control) promoters was tested by ChIP assays. RNA pol II's DNA binding to the *gapdh* promoter was used as an internal control. The DO-1mAb was used to immunoprecipitate p53. (**e**) Vanadate and DMHV directly inhibit the DNA-binding activity of recombinant GST-p53. Recombinant p53 was preincubated for 30 min at 37°C in the presence or absence of the indicated concentrations of inhibitors, and DNA-binding reactions were performed using the [^{32}P]-labeled oligonucleotide probe, in the presence of the p53 rabbit polyclonal antibody. To ascertain the specificity of GST-p53 for the oligonucleotide probe, competition assays were also performed (lanes 3 and 4). W and M denote unlabeled wild-type and mutant oligonucleotide competitors, respectively

because reports have variously stated that vanadate suppresses,[26,27] enhances,[28–30] or induces[31] apoptosis. This may be due to differences in the genetic background of the experimental materials, such as the cells' p53 status, and in the apoptotic stimuli used in these studies. In these reports, there is no information about the p53 status of the cell lines used. We observed the induction and enhancement of p53-independent apoptosis by vanadate in irradiated HL60, U937, and MOLT/p53KD cells (especially MOLT/p53KD-2) (Figure 4b and e). One explanation for this effect may be that the SAPK/JNK-dependent apoptotic pathway is augmented, because the loss of p53 function potentiates this pathway[32] and vanadate enhances it (Figure 4c). Such augmentation, like the upregulation of SAPK/JNK phosphorylation, was observed in these cells when they were treated with vanadate alone (data not shown). This probably contributes to the slight cytotoxic effect of vanadate on MOLT-4 cells (Figures 1c and 4a). Thus, considering the relative contributions of p53 and SAPK/JNK, p53 seems to dominate in irradiated MOLT-4 cells.

It is well known that p53 is regulated by post-translational modifications, including phosphorylation and acetylation;[10] however, vanadate does not alter p53's phosphorylation status (Figure 7) or any acetylation status tested (data not shown). The lack of effect of vanadate on the p53 phosphorylation seems to be in accord with its lack of effect on p53 accumulation (Figures 4d and 5a). These data do not completely rule out the possibility that there is an alteration of p53 at other Ser/Thr phosphorylation sites besides the six residues investigated; however, considering the evidence that vanadate does not require enzymes to inhibit the DNA-binding activity of p53 (Figure 8e), it is reasonable to conclude that vanadate's effect does not require any enzyme-dependent modifications, such as phosphorylation. Thus, we propose that vanadate inactivates p53 by inducing a conformational change in it. Interestingly, besides our study, Landesman *et al*.[22] have described *in vitro* epitopic changes in p53 by vanadate, using a very similar immunoprecipitation analysis with PAb 240 mAb. They reported that the conformational change can be induced in cell lysates by adding vanadate to a 1 mM final concentration; however, we did not observe this change in immunoreactivity when vanadate was simply added to the buffers (see Materials and Methods) (Figure 8a, 4th lane). In our study, vanadate required *in vivo* warm incubation for PAb 240 mAb to immunoprecipitate p53 (Figure 8a, 5th lane). This difference may involve the presence or the absence of the SV40 large T antigen, since they used a cell line (SV80) that contains it and MOLT-4 cells do not. Interestingly, Kernohan *et al*.[23] have reported that metal ions such as zinc modify the p53–T-antigen complex formation, using mAbs that recognize the conformationally changed p53. Thus, vanadate may also alter the complex formation and induce the conformational change of p53 more easily in the presence of T antigen than in its absence. Although the mechanism of the change they observed might be different from the one we observed, their study was the first to deal with the effect of vanadate on the p53 molecule itself. In this respect, it is known that p53 has a metal-binding feature and is inactivated by exposure to cadmium ions.[24,33] Accordingly, we propose that the metal-binding site in p53 may be targeted by the vanadate anion(s).

Finally, several studies have implicated vanadium as a carcinogen.[34,35] Therefore, the inhibitory effect of vanadate on p53 may be associated with vanadate's carcinogenesis, since the loss of p53 function predisposes mice to cancer.[36] On the other hand, vanadate may be useful for inhibiting DNA damage-induced apoptosis, as a radioprotector, or for inhibiting the side effects of cancer therapy. Several researchers have identified chemical inhibitors of p53, such as pifithrin,[37] cadmium,[24,33] and salicylate.[38] Among these inhibitors, pifithrin inhibits the nuclear localization of p53 after DNA damage, but cadmium and salicylate inhibit the DNA-binding activity of p53. Vanadate weakly inhibits the nuclear localization of p53, and potently inhibits the DNA-binding activity of p53. It is noteworthy that pifithrin protects mice from lethal γ-ray exposure.[37] Thus, p53 inhibitors are useful for reducing genotoxic stress. Further studies are warranted to investigate vanadate's usefulness for protecting cells from DNA damage-induced apoptosis.

Materials and Methods

Cell culture and treatment

The human T-cell leukemia cell line MOLT-4, the human acute promyelocytic leukemia cell line HL60, the human monoblastic lymphoma cell line U937, and MOLT-4 stable transfectants overexpressing the murine Bcl-2 (MOLT/mBcl-2),[2] short hairpin (sh)-type p53 small interfering RNA (siRNA) (MOLT/p53KD-1, -2), and the negative control shRNA (MOLT/Nega) were cultured in RPMI 1640 medium (Sigma) supplemented with 10% fetal bovine serum (FBS, Hyclone). The murine IL-3-dependent pro-B cell line Ba/F3 was cultured as previously described.[18] The murine mammary carcinoma cell line FM3A was cultured in Eagle's minimal essential medium (Sigma) supplemented with 5% FBS. Cells were maintained at 37°C in a humidified atmosphere containing 5% CO_2. To generate stable transfectants (MOLT/p53KD-1, -2 and MOLT/Nega), MOLT-4 cells were transfected by electroporation (Gene Pulsar II, Bio-Rad; 0.25 kV, 950 microfarads) with the *ApaLI*-linearized vectors (GeneSuppressor System, p53 siRNA plasmid and the negative control shRNA plasmid, IMGENEX), and selected on 0.16% soft agar culture containing 0.8 mg/ml G418 for 3 weeks. Exponentially growing cell cultures (5×10^5 cells/ml) in tissue culture dishes or flasks (Becton Dickinson) were irradiated at room temperature with an X-ray generator (Pantak HF 350, Shimadzu) operating at 200 kV–20 mA with a filter of 0.5 mm Cu and 1 mm Al at dose rate of 1.46 or 2.92 Gy/min. Cell density was determined with a cell counter (Z1 Cell and particle counter, Beckman Coulter). Vanadate (Wako, Japan) was prepared at a concentration of 0.5 M according to the method of Gordon.[13] Z-VAD-FMK (Kamiya Biomedical Company), DMHV (Calbiochem), DPS (Calbiochem), PAO (Sigma), Etoposide (Wako), and Anisomycin (Calbiochem) were dissolved in dimethyl sulfoxide (Me_2SO) at concentrations of 20 mM, 25 mM, 10 mM, 0.4 mM, 10 mM, and 2 mg/ml, respectively. These reagents were added to the culture medium immediately after IR unless otherwise specified. Protein concentrations were determined using Coomassie Plus Protein Assay Reagent (Pierce).

Caspase activity

N-Acetyl-Asp-Glu-Val-Asp-*p*-nitroanilide (Ac-DEVD-pNA, Biomol) at a concentration of 200 μM was incubated with 250 ng/ml recombinant active caspase-7 (Medical and Biological Laboratories (MBL), Japan) for 30 min

at 37°C in the presence or absence of the indicated concentrations of vanadate in reaction buffer containing 20 mM PIPES-NaOH, pH 7.2, 100 mM NaCl, 0.1% CHAPS, and 10% sucrose with or without 10 mM DTT. Control reactions were supplemented with vehicle Me_2SO instead of 10 mM Ac-DEVD-pNA solution. These reactions were stopped by chilling on ice. The concentration of hydrolyzed *p*-nitroaniline was quantified by measuring the absorbance at 385 nm in a spectrophotometer (Shimadzu).

Flow cytometric analysis

All samples were counted and over 5000 cells analyzed with a flow cytometer (EPICS XL System II, Beckman Coulter). Cell viability was determined by Annexin V-FITC and propidium iodide (PI) staining using a MEBCYTO Apoptosis Kit (MBL). Viability was defined as the percentage of Annexin V-negative and PI-negative cells. The percentage of cells losing their $\Delta\psi m$ was determined by MitoTracker staining. Cells were incubated in culture medium for 30 min at 37°C with 100 nM MitoTracker Red CMXRos dye (Molecular Probes) to mark the mitochondria. The cells were then washed once, suspended in ice-cold phosphate-buffered saline (PBS), and analyzed by flow cytometer.

The conformational change of Bax was measured by immunofluorescence staining with an anti-Bax mAb (clone 4F11, MBL). One million cells washed once with ice-cold PBS containing 2% FBS (PBS-F) were fixed with 200 μl of 4% paraformaldehyde in 0.1 M NaH_2PO_4, pH 7.4 for 10 min on ice, and then washed twice with PBS-F. All the Bax staining procedures described below were performed at room temperature. Fixed cells were permeabilized with 200 μl of PBS containing 100 μg/ml digitonin (Wako) for 10 min, and then washed twice with PBS-F. Permeabilized cells were subjected to blocking with 10 μl of normal rabbit serum for 5 min, 40 μl of 10 μg/ml anti-Bax mAb in PBS-F was added to the cell suspension, and the suspension was then incubated for 30 min. The cells were washed twice with PBS-F, suspended with 40 μl of a 1 : 160 dilution of FITC-labeled anti-mouse IgG (Fc) secondary antibody (MBL), incubated for 30 min, washed twice with PBS-F, and suspended in 500 μl of PBS. After these treatments, the fluorescence intensity of each cell was analyzed by flow cytometer.

Subcellular fractionation to measure the release of Cyt.*c*, Smac/DIABLO, and Histone H1

All extraction steps were carried out at 4°C. Twenty million cells were washed twice with PBS and suspended in 50 μl of isotonic buffer (10 mM HEPES-NaOH, pH 7.4, 0.3 M Mannitol, 0.1% BSA). The cell suspensions were mixed with 50 μl of isotonic buffer containing 200 μM digitonin, incubated for 5 min, and then spun at 10 000 $\times$ *g* for 4 min. The resulting supernatants were collected and mixed with an equal volume of 2 $\times$ SDS-PAGE sample buffer (125 mM Tris-HCl, pH 6.8, 2% sodium lauryl sulfate (SDS), 10% glycerol, 6% β-mercaptoethanol, 0.01% crystal violet). The mixtures were boiled for 10 min, and spun at 20 000 $\times$ *g* for 10 min at room temperature. After the centrifugation, the final supernatants were used as the cytosolic fractions for the immunoblotting described below.

Immunoblotting analysis

Two million cells washed once with ice-cold PBS were lysed in 100 μl of 1 $\times$ SDS-PAGE sample buffer, and boiled for 10 min. After centrifugation at 20 000 $\times$ *g* for 10 min at room temperature, the supernatant was collected as the loading sample, and then 2–20 μl of the loading samples or cytosolic fractions were separated by electrophoresis through an SDS-polyacrylamide gel. Proteins in the gel were subjected to electrophoretic semidry transfer to a polyvinylidene difluoride membrane (Millipore). The membranes were blocked with 1% BSA, 5% nonfat milk, or 0.5% Blocking Reagent in TBS-T (20 mM Tris-HCl, pH 7.5, 150 mM NaCl, 0.05% Tween 20) for 1 h at room temperature. Blocking Reagent (Roche) was used in the case of phosphotyrosine detection. These blocked membranes were incubated overnight at 4°C with antibody against caspase-7 (MBL), cleaved caspase-3 (active caspase-3) (Cell Signaling), caspase-9 (MBL), Cyt.*c* (BD Pharmingen), Smac (MBL), β-actin (Sigma), Bax (clone 4F11, MBL), human p53 (clone DO-1, Santa Cruz Biotechnology), murine p53 (clone PAb 240, Calbiochem), p21 (Calbiochem), PUMA (Calbiochem), Histone H1 (clone AE-4, Upstate), phosphotyrosine (clone 4G10, Upstate), phospho-p53 (Phospho-p53 antibody sampler kit, Cell Signaling), or Ku70[39] as primary antibodies. Since the anti-p53 (DO-1) and -phosphotyrosine (4G10) antibodies were peroxidase conjugated, they did not require a secondary antibody for visualization. For the other antibodies, the membranes were then washed four times with TBS-T followed by incubation for 2 h at room temperature with peroxidase-conjugated antibody against rabbit or mouse IgG (Dako) as the secondary antibody. The membranes were then washed three times with TBS-T, washed twice with TBS (20 mM Tris-HCl, pH 7.5, 150 mM NaCl), and developed using a Konica Immunostaining HRP-1000 kit (Konica, Japan), or ECL-plus kit (Amersham Biosciences). In the case of the ECL-plus kit, the signals were obtained by exposure to X-ray films (Hyperfilm MP, Amersham Biosciences) or using a luminescence image analyzing system (LAS-1000 mini, Fujifilm, Japan).

Semiquantitative RT-PCR analysis

The isolation of total RNA from cells was performed using the Ultraspec RNA isolation system (Biotecx) according to the manufacturer's instructions. RNAs were converted to cDNAs using MMLV reverse transcriptase (Life Technologies) and oligo$(dT)_{12\text{-}18}$ (Amersham Biosciences). The cDNA was then amplified by polymerase chain reaction (PCR) using AmpliTaq Gold DNA polymerase (Applied Biosystems). The primer sequences were as follows: *p21*, (forward) 5′-GTTCCTTGTGGAGCCGGAGC-3′, (reverse) 5′-GGTACAAGACAGTGACAGGTC-3′; *puma*, (forward) 5′-TGTAGAGGAGACAGGAATCCACGG-3′, (reverse) 5′-AGGCACCTAATTGGGCTCCATCTC-3′; *β-actin*, (forward) 5′-TGACGGGGTCACCCACACTGTGCCCATCTA-3′, (reverse) 5′-CTAGAACATTTGCGGTGGACGATGGAGGG-3′. After heat denaturation for 9 min at 95°C, each PCR amplification for 25 cycles (for *p21*, *β-actin*) and 37 cycles (for *puma*) was performed as follows: 40 s at 94°C, 1 min at 60–62°C, and 40 s at 72°C except that, in the last cycle, extension was carried out for 6 min 40 s, in a GeneAmp PCR system 2400 (Perkin Elmer). The RT-PCR products were separated by electrophoresis through a 1.5 or 2% agarose gel, stained with ethidium bromide, and visualized by UV emission.

Immunoprecipitation of p53

Anti-p53 DO-1-conjugated agarose (Calbiochem) and anti-p53 PAb 240 (Calbiochem) were used to immunoprecipitate p53 from MOLT-4 extracts. Ten million MOLT-4 cells were washed once with ice-cold PBS containing 1 mM vanadate, and lysed in 1 ml of ice-cold TNEV buffer (10 mM Tris-HCl, pH 7.8, 1% NP40, 1 mM EDTA, 1 mM vanadate, 150 mM NaCl, 10 μg/ml aprotinin) for 15 min on ice. MOLT-4 extracts were obtained by centrifugation at 20 000 $\times$ *g* for 15 min at 4°C. Proteins were immunoprecipitated overnight at 4°C. Protein G plus agarose (Calbiochem) was added to the PAb 240 mixture and incubated for another 2 h to precipitate

the PAb 240 immunocomplex and inactivated p53. All the beads were collected by centrifugation, and then washed four times with ice-cold TNEV buffer. After the wash, the proteins were released by adding 1 × SDS-PAGE sample buffer, and the samples were spun at 20 000 × *g* for 10 min at room temperature. The final supernatants were subjected to immunoblotting. In the case of the [^{32}P]-labeling experiment, irradiated or unirradiated MOLT-4 cells were suspended in sodium dihydrogenphosphate-deprived medium (D-MEM, Invitrogen (Gibco)) and supplemented with 10% fetal bovine serum that had been dialyzed against 0.15 M NaCl (Invitrogen (Gibco)). The cells were then treated with vanadate (1 mM) or left untreated, and then with $H_3^{32}PO_4$ (11.1 MBq (300 μCi)/ml) (Perkin Elmer). After these treatments, the cells were incubated at 37°C in a humidified atmosphere containing 5% CO_2. They were harvested 6 h after IR for the immunoprecipitation of [^{32}P]-labeled p53.

Preparation of nuclear extracts and gel-shift assays

All extraction steps were carried out at 4°C. Thirty million MOLT-4 cells were washed once with PBS and suspended in 200 μl of hypotonic buffer A (20 mM HEPES-NaOH, pH 7.9, 10 mM KCl, 1 mM $MgCl_2$, 0.5 mM PMSF, 0.5 mM DTT) to rupture the cells, and the suspension was incubated for 10 min. Nuclear pellets were obtained by centrifugation at 1000 × *g* for 10 min. The pellets were resuspended in 40 μl of high-salt buffer B (20 mM HEPES-NaOH, pH 7.9, 400 mM KCl, 1 mM $MgCl_2$, 5% glycerol, 0.5 mM PMSF, 0.5 mM DTT), subjected to three freeze-thaw cycles, and then mixed with 120 μl of dilution buffer C (20 mM HEPES-NaOH, pH 7.9, 1 mM $MgCl_2$, 5% glycerol, 0.5 mM PMSF, 0.5 mM DTT). These suspensions were spun at 20 000 × *g* for 15 min. The protein concentrations of the resulting supernatants were equalized at 1 μg/μl with dilution buffer D (20 mM HEPES-NaOH, pH 7.9, 100 mM KCl, 1 mM $MgCl_2$, 5% glycerol, 0.5 mM PMSF, 0.5 mM DTT). These nuclear extracts were stored at −80°C. Gel-shift and super-shift assays were performed using a Nushift p53 kit (Active Motif) according to the manufacturer's instructions. The reaction mixtures were essentially as follows: For gel-shift, 0.5 μl of [^{32}P]-labeled oligonucleotide probe and the indicated amounts of nuclear extract/12 μl of reaction mixture/lane; for super-shift, 0.5 μl of p53 rabbit polyclonal antibody supplied with the kit, 0.5 μl of [^{32}P]-labeled oligonucleotide probe, and the indicated amounts of nuclear extract/12 μl of reaction mixture/lane. The sequence of the oligonucleotide probe supplied with the kit contains 19-mer p53 ideal consensus-binding site. Reaction mixtures were incubated for 20 min at 25°C, and then separated by electrophoresis through a 5% polyacrylamide gel with TGE buffer (50 mM Tris, 380 mM glycine, 2.1 mM EDTA) at 4°C. The results were quantified by densitometry using Image Gauge version 4.21 software (Fujifilm). The protocol for the DNA-binding assays using recombinant GST-p53[40] was as follows: GST-p53 (25 ng) was preincubated for 30 min at 37°C in the presence or absence of the indicated concentrations of vanadate in 10 μl of binding buffer containing 20 mM HEPES-NaOH, pH 8.2, 100 mM KCl, 50 μM DTT, 0.3 ng/μl sonicated salmon sperm DNA, 0.5 μg/μl bovine serum albumin, 5% glycerol, and 0.1% CHAPS. For competition experiments, 2.5 ng/μl of the unlabeled wild-type or mutant oligonucleotide supplied with the kit was included in the reaction mixture. The wild-type competitor oligonucleotide sequence was identical to the [^{32}P]-labeled oligonucleotide sequence, and the mutant competitor oligonucleotide contained a 4-mer mutation within the p53 consensus binding site. The samples were then mixed with 0.5 μl of the p53 rabbit polyclonal antibody and 0.5 μl of [^{32}P]-labeled oligonucleotide probe and incubated for 20 min at 4°C. The reaction mixtures (11 μl of the total volume/lane) were then separated by electrophoresis at 4°C.

ChIP assays

For the ChIP assays, 5 × 10^6 MOLT-4 cells were fixed 4 h after 10 Gy IR, with 0.6% formaldehyde for 5 min at 37°C. Cells were washed twice with PBS containing protease inhibitors (1 mM PMSF, 1 μg/ml aprotinin, and 1 μg/ml pepstatin A), and then lysed in 1 ml of SDS lysis buffer (50 mM Tris-HCl, pH 8.1, 1% SDS, 10 mM EDTA, 1 mM PMSF, 1 μg/ml aprotinin, 1 μg/ml pepstatin A) for 10 min on ice. To shear the DNA into lengths between 200 and 1000 bp, the lysates were sonicated with six sets of 20-s pulses using a Branson, SONIFIER B-12, 150 W model at 20% of maximum power. These sonicated lysates were spun at 10 000 × *g* for 10 min, and the resulting supernatants were divided into 200 μl aliquots. Each 200 μl aliquot was diluted 10-fold in ChIP dilution buffer (16.7 mM Tris-HCl, pH 8.1, 167 mM NaCl, 0.01% SDS, 1.1% Triton X-100, 1.2 mM EDTA, 1 mM PMSF, 1 μg/ml aprotinin, 1 μg/ml pepstatin A). Samples (2 ml) of diluted cell supernatant were subjected to the ChIP assay. The ChIP assay was performed using a ChIP assay kit (Upstate) according to the manufacturer's instructions. The particular specifications were as follows: 1 μg DO-1 mAb (Calbiochem) and 4H8 mAb (Active Motif) were used to immunoprecipitate p53 and RNA polymerase II (RNA pol II), respectively, from each ChIP sample. Phenol/chloroform-extracted ChIP sample DNA was precipitated with isopropyl alcohol and an inert carrier (Pellet Paint Co-Precipitant, Novagen). The p53-associated or RNA pol II-associated DNA was then amplified by PCR using platinum *Pfx* DNA polymerase (Invitrogen). The promoter-specific primer sequences were as follows: *p21* (forward) 5′-GTGGCTCTGATTGGCTTTCTGGC-3′ (reverse) 5′-GCTCACCACCACCACGACATTCA-3′; *puma* (forward) 5′-TTGCGA GACTGTGGCCTTGTGTC-3′ (reverse) 5′-GTCGGACACACACACTGA CTGGGA-3′; *gapdh* (forward) 5′-TACTAGCGGTTTTACGGGCG-3′ (reverse) 5′-TCGAACAGGAGGAGCAGAGAGCGA-3′. After heat denaturation for 1.5 min at 98°C, each PCR amplification for 35 cycles (for *p21*) or 33 cycles (for *puma*, *gapdh*) was performed as follows: 15 s at 98°C and 30 s at 68°C, except that, in the last cycle, extension was carried out for 6 min 30 s, in a GeneAmp PCR system 9700 (Applied Biosystems). The PCR products were separated by electrophoresis through a 2% agarose gel, stained with ethidium bromide, and visualized by UV emission.

Acknowledgements

We thank all the members of our laboratory for their help and encouragement. We also thank Dr. T Shibue and Professor T Taniguchi (University of Tokyo) for their kind gift of the Ba/F3 cells, and Dr. M Enari (National Cancer Center, Tokyo, Japan) for various suggestions and instructions, especially regarding the ChIP assays. This work was supported in part by grants from the Ministry of Education, Science, Sports and Culture, the Ministry of Health and Welfare of Japan.

References

1. Nakano H, Kohara M and Shinohara K (2001) Evaluation of the relative contribution of p53-mediated pathway in X-ray-induced apoptosis in human leukemic MOLT-4 cells by transfection with a mutant p53 gene at different expression levels. Cell Tissue Res. 306: 101–106
2. Enomoto A, Suzuki N, Hirano K, Matsumoto Y, Morita A, Sakai K and Koyama H (2000) Involvement of SAPK/JNK pathway in X-ray-induced rapid cell death of human T-cell leukemia cell line MOLT-4. Cancer Lett. 155: 137–144
3. Enomoto A, Suzuki N, Kang Y, Hirano K, Matsumoto Y, Zhu J, Morita A, Hosoi Y, Sakai K and Koyama H (2003) Decreased *c*-Myc expression and its involvement in X-ray-induced apoptotic cell death of human T-cell leukemia cell line MOLT-4. Int. J. Radiat. Biol. 79: 589–600

4. Morita A, Suzuki N, Matsumoto Y, Hirano K, Enomoto A, Zhu J and Sakai K (2000) p41 as a possible marker for cell death is generated by caspase cleavage of p42/SETβ in irradiated MOLT-4 cells. Biochem. Biophys. Res. Commun. 278: 627–632
5. Morimatsu A, Suzuki N, Hirano K, Matsumoto Y and Sakai K (1996) Identification and characterization of a protein found after X-irradiation in human T cell leukemia. J. Radiat. Res. 37: 1–11
6. Hengartner MO (2000) The biochemistry of apoptosis. Nature 407: 770–776
7. Zheng TS, Hunot S, Kuida K and Flavell RA (1999) Caspase knockouts: matters of life and death. Cell Death Differ. 6: 1043–1053
8. Roucou X and Martinou JC (2001) Conformational change of Bax: a question of life or death. Cell Death Differ. 8: 875–877
9. Desagher S, Osen-Sand A, Nichols A, Eskes R, Montessuit S, Lauper S, Maundrell K, Antonsson B and Martinou JC (1999) Bid-induced conformational change of Bax is responsible for mitochondrial cytochrome *c* release during apoptosis. J. Cell Biol. 144: 891–901
10. Wahl GM and Carr AM (2001) The evolution of diverse biological responses to DNA damage: insights from yeast and p53. Nature Cell Biol. 3: E277–E286
11. Villunger A, Michalak EM, Coultas L, Mullauer F, Bock G, Ausserlechner MJ, Adams JM and Strasser A (2003) p53- and drug-induced apoptotic responses mediated by BH3-only proteins Puma and Noxa. Science 302: 1036–1038
12. Konishi A, Shimizu S, Hirota J, Takao T, Fan Y, Matsuoka Y, Zhang L, Yoneda Y, Fujii Y, Skoultchi AI and Tsujimoto Y (2003) Involvement of Histone H1.2 in apoptosis induced by DNA double-strand breaks. Cell 114: 673–688
13. Gordon JA (1991) Use of vanadate as protein-phosphotyrosine phosphatase inhibitor. Methods Enzymol. 201: 477–482
14. Cuncic C, Desmarais S, Detich N, Tracey AS, Gresser MJ and Ramachandran C (1999) Bis(*N,N*-dimethylhydroxamido)hydrooxovanadate inhibition of protein tyrosine phosphatase activity in intact cells: comparison with vanadate. Biochem. Pharmacol. 58: 1859–1867
15. Fujiwara S, Watanabe T, Nagatsu T, Gohda J, Imoto M and Umezawa K (1997) Enhancement or induction of neurite formation by a protein tyrosine phosphatase inhibitor, 3,4-Dephostatin, in growth factor-treated PC12 h cells. Biochem. Biophys. Res. Commun. 238: 213–217
16. Pasquet JM, Dachary-Prigent J and Nurden AT (1998) Microvesicle release is associated with extensive protein tyrosine dephosphorylation in platelets stimulated by A23187 or a mixture of thrombin and collagen. Biochem. J. 333: 591–599
17. Saito Y, Mitsuhashi N, Sakurai H, Ishikawa H, Hasegawa M, Akimoto T, Hayakawa K and Niibe H (1999) Apoptosis and appearance of Trp53-positive micronuclei in murine tumors with different radioresponses *in vivo*. Radiat. Res. 152: 462–467
18. Mathieu AL, Gonin S, Leverrier Y, Blanquier B, Thomas J, Dantin C, Martin G, Baverel G and Marvel J (2001) Activation of the phosphatidylinositol 3-kinase/Akt pathway protects against interleukin-3 starvation but not DNA damage-induced apoptosis. J. Biol. Chem. 276: 10935–10942
19. Shimizu T and Pommier Y (1997) Camptothecin-induced apoptosis in p53-null human leukemia HL60 cells and their isolated nuclei: effects of the protease inhibitors Z-VAD-fmk and dichloroisocoumarin suggest an involvement of both caspases and serine proteases. Leukemia 11: 1238–1244
20. Sugimoto K, Toyoshima H, Sakai R, Miyagawa K, Hagiwara K, Ishikawa F, Takaku F, Yazaki Y and Hirai H (1992) Frequent mutations in the p53 gene in human myeloid leukemia cell lines. Blood 79: 2378–2383
21. Harris N, Brill E, Shohat O, Prokocimer M, Wolf D, Arai N and Rotter V (1986) Molecular basis for heterogeneity of the human p53 protein. Mol. Cell. Biol. 6: 4650–4656
22. Landesman Y, Bringold F and Kimchi A (1994) p53 undergoes epitopic changes *in vitro* by sodium-vanadate. Oncogene 9: 1241–1245
23. Kernohan NM, Hupp TR and Lane DP (1996) Modification of an N-terminal regulatory domain of T antigen restores p53-T antigen complex formation in the absence of an essential metal ion cofactor. J. Biol. Chem. 271: 4954–4960
24. Meplan C, Mann K and Hainaut P (1999) Cadmium induces conformational modifications of wild-type p53 and suppresses p53 response to DNA damage in cultured cells. J. Biol. Chem. 274: 31663–31670
25. Baliga B and Kumar S (2003) Apaf-1/cytochrome *c* apoptosome: an essential initiator of caspase activation or just a sideshow? Cell Death Differ. 10: 16–18
26. Lawson AE, Bao H, Wickrema A, Jacobs-Helber SM and Sawyer ST (2000) Phosphatase inhibition promotes antiapoptotic but not proliferative signaling pathways in erythropoietin-dependent HCD57 cells. Blood 96: 2084–2092
27. Chin LS, Murray SF, Harter DH, Doherty PF and Singh SK (1999) Sodium vanadate inhibits apoptosis in malignant glioma cells: a role for Akt/PKB. J. Biomed. Sci. 6: 213–218
28. Gamero AM and Larner AC (2001) Vanadate facilitates interferon α-mediated apoptosis that is dependent on the Jak/Stat pathway. J. Biol. Chem. 276: 13547–13553
29. Stewart CE, Mihai R and Holly JM (1999) Increased tyrosine kinase activity but not calcium mobilization is required for ceramide-induced apoptosis. Exp. Cell Res. 250: 329–338
30. Guo YL, Baysal K, Kang B, Yang LJ and Williamson JR (1998) Correlation between sustained *c*-Jun N-terminal protein kinase activation and apoptosis induced by tumor necrosis factor- in rat mesangial cells. J. Biol. Chem. 273: 4027–4034
31. Figiel I and Kaczmarek L (1997) Orthovanadate induces cell death in rat dentate gyrus primary culture. Neuroreport 8: 2465–2470
32. Huang S, Shu L, Dilling MB, Easton J, Harwood FC, Ichijo H and Houghton PJ (2003) Sustained activation of the JNK cascade and rapamycin-induced apoptosis are suppressed by p53/p21^{Cip1}. Mol. Cell 11: 1491–1501
33. Meplan C, Verhaegh G, Richard MJ and Hainaut P (1999) Metal ions as regulators of the conformation and function of the tumour suppressor protein p53: implications for carcinogenesis. Proc. Nutr. Soc. 58: 565–571
34. Ress NB, Chou BJ, Renne RA, Dill JA, Miller RA, Roycroft JH, Hailey JR, Haseman JK and Bucher JR (2003) Carcinogenicity of inhaled vanadium pentoxide in F344/N rats and B6C3F$_1$ Mice. Toxicol. Sci. 74: 287–296
35. Sakai A (1997) Orthovanadate, an inhibitor of protein tyrosine phosphatases, acts more potently as a promoter than as an initiator in the BALB/3T3 cell transformation. Carcinogenesis 18: 1395–1399
36. Donehower LA, Harvey M, Slagle BL, McArthur MJ, Montgomery Jr CA, Butel JS and Bradley A (1992) Mice deficient for p53 are developmentally normal but susceptible to spontaneous tumours. Nature 356: 215–221
37. Komarov PG, Komarova EA, Kondratov RV, Christov-Tselkov K, Coon JS, Chernov MV and Gudkov AV (1999) A chemical inhibitor of p53 that protects mice from the side effects of cancer therapy. Science 285: 1733–1737
38. Chernov MV and Stark GR (1997) The p53 activation and apoptosis induced by DNA damage are reversibly inhibited by salicylate. Oncogene 14: 2503–2510
39. Sakata K, Matsumoto Y, Tauchi H, Satoh M, Oouchi A, Nagakura H, Koito K, Hosoi Y, Suzuki N, Komatsu K and Hareyama M (2001) Expression of genes involved in repair of DNA double-strand breaks in normal and tumor tissues. Int. J. Radiat. Oncol. Biol. Phys. 49: 161–167
40. Komiyama S, Taniguchi S, Matsumoto Y, Tsunoda E, Ohto T, Suzuki Y, Yin HL, Tomita M, Enomoto A, Morita A, Suzuki T, Ohtomo K, Hosoi Y and Suzuki N (2004) Potentiality of DNA-dependent protein kinase to phosphorylate Ser46 of human p53. Biochem. Biophys. Res. Commun. 323: 816–822